

MIT Open Access Articles

*Fucosylation Deficiency in Mice
Leads to Colitis and Adenocarcinoma*

The MIT Faculty has made this article openly available. **Please share** how this access benefits you. Your story matters.

Citation: Wang, Yiwei et al. "Fucosylation Deficiency in Mice Leads to Colitis and Adenocarcinoma." *Gastroenterology* 152, 1 (January 2017): 193–205 © 2017 AGA Institute Background & Aims

As Published: <http://dx.doi.org/10.1053/J.GASTRO.2016.09.004>

Publisher: Elsevier BV

Persistent URL: <http://hdl.handle.net/1721.1/117652>

Version: Final published version: final published article, as it appeared in a journal, conference proceedings, or other formally published context

Terms of use: Creative Commons Attribution-NonCommercial-NoDerivs License





Published in final edited form as:

Gastroenterology. 2017 January ; 152(1): 193–205.e10. doi:10.1053/j.gastro.2016.09.004.

Fucosylation Deficiency in Mice Leads to Colitis and Adenocarcinoma

Yiwei Wang¹, Dan Huang¹, Kai-Yuan Chen², Min Cui¹, Weihuan Wang¹, Xiaoran Huang¹, Amad Awadallah³, Qing Li³, Ann Friedman⁴, William W. Xin⁵, Luca Di Martino⁶, Fabio Cominelli⁶, Alex Miron⁷, Ricky Chan⁸, James Fox⁹, Yan Xu¹⁰, Xiling Shen², Mathew F. Kalady¹¹, Sanford Markowitz¹², Ivan Maillard⁴, John B. Lowe¹³, Wei Xin^{1,3}, and Lan Zhou^{1,3}

¹Department of Pathology, Case Western Reserve University, Cleveland, OH 44106, USA

²Department of Biomedical Engineering, Cornell University, Ithaca, NY 14853, USA

³Department of Pathology, University Hospitals Case Medical Center, Cleveland, OH 44106, USA

⁴Life Sciences Institute, University of Michigan, Ann Arbor, MI 48109, USA

⁵School of Arts & Sciences, University of Pennsylvania, Philadelphia, PA, 19104-6304, USA

⁶Department of Internal Medicine, University Hospitals Case Medical Center, Cleveland, OH 44106, USA

⁷Department of Genetics and Genome Sciences, Case Western Reserve University, Cleveland, OH 44106, USA

⁸Institute for Computational Biology, Case Western Reserve University, Cleveland, OH 44106, USA

⁹Division of Comparative Medicine, Massachusetts Institute of Technology, Cambridge, Massachusetts, USA

¹⁰Department of Chemistry, Cleveland State University, Cleveland, OH 44106, USA

¹¹Department of Colorectal Surgery, Digestive Diseases Institute, Cleveland Clinic, Cleveland, OH 44106, USA

¹²Department of Medicine, Case Western Reserve University, Cleveland, OH 44106, USA

Correspondence: Lan Zhou, Department of Pathology, Case Western Reserve University, Cleveland, OH 44106; lan.zhou@case.edu, Tel:(216)3681671.

Disclosure of potential conflicts of interest: The authors declare no potential conflicts relevant to the manuscript

Author contributions: Study concept and design: J. Lowe, W. Xin, L. Zhou

Acquisition of data: Y. Wang, M. Cui, W. Wang, KY Chen, D. Huang, X. Huang, A. Amadallah, Q. Li, L. Di Martino, W.W. Xin, R. Chan, Y. Xu, J. Fox, X. Shen, M. F. Kalady, W. Xin, L. Zhou

Analysis and interpretation of data: Y. Wang, M. Cui, KY Chen, D. Huang, F. Cominelli, R. Chan, J. Fox, S. Markowitz, M. F. Kalady, J. Lowe, W. Xin, L. Zhou

Drafting of the manuscript: Y. Wang, J. Lowe, W. Xin, L. Zhou

Critical revision of the manuscript for important intellectual content: Fabio Cominelli, S. Markowitz, J. Lowe, W. Xin, L. Zhou

Author names in bold designate shared co-first authorship

Publisher's Disclaimer: This is a PDF file of an unedited manuscript that has been accepted for publication. As a service to our customers we are providing this early version of the manuscript. The manuscript will undergo copyediting, typesetting, and review of the resulting proof before it is published in its final citable form. Please note that during the production process errors may be discovered which could affect the content, and all legal disclaimers that apply to the journal pertain.

¹³Department of Pathology, Genentech Inc., San Francisco, CA, 94080 USA

Abstract

Background & Aims—De novo synthesis of GDP-fucose, a substrate for fucosylglycans, requires sequential reactions mediated by GDP-mannose 4,6-dehydratase (GMDS) and GDP-4-keto-6-deoxymannose 3,5-epimerase-4-reductase (FX or TSTA3). GMDS deletions and mutations are found in 6%–13% of colorectal cancers; these mostly affect ascending and transverse colon. We investigated whether lack of fucosylation consequent to loss of GDP-fucose synthesis contributes to colon carcinogenesis.

Methods—FX deficiency and GMDS deletion produce the same biochemical phenotype of GDP-fucose deficiency. We studied a mouse model of fucosylation deficiency (*Fx*^{-/-} mice) and mice with the full-length *Fx* gene (controls). Mice were placed on standard chow or fucose-containing diet (equivalent to a control fucosylglycan phenotype). Colon tissues were collected and analyzed histologically or by ELISAs to measure cytokine levels; T cells were also collected and analyzed. Fecal samples were analyzed by 16s rRNA sequencing. Mucosal barrier function was measured by uptake of fluorescent dextran. We transplanted bone marrow cells from *Fx*^{-/-} or control mice (Ly5.2) into irradiated 8-week old *Fx*^{-/-} or control mice (Ly5.1). We performed immunohistochemical analyses for expression of Notch and the *hes* family bHLH transcription factor (HES1) in colon tissues from mice and a panel of 60 human colorectal cancer specimens (27 left-sided, 33 right-sided).

Results—*Fx*^{-/-} mice developed colitis and serrated-like lesions. The intestinal pathology of *Fx*^{-/-} mice was reversed by addition of fucose to the diet, which restored fucosylation via a salvage pathway. In the absence of fucosylation, dysplasia appeared and progressed to adenocarcinoma in up to 40% of mice, affecting mainly the right colon and cecum. Notch was not activated in *Fx*^{-/-} mice fed standard chow, leading to decreased expression of its target *Hes1*. Fucosylation deficiency altered the composition of the fecal microbiota, reduced mucosal barrier function and altered epithelial proliferation marked by Ki67. *Fx*^{-/-} mice receiving control bone marrow cells had intestinal inflammation and dysplasia, and reduced expression of cytokines produced by cytotoxic T cells. Human sessile serrated adenomas and right-sided colorectal tumors with epigenetic loss of MLH1 had lost or had lower levels of HES1 than other colorectal tumor types or nontumor tissues.

Conclusions—In mice, fucosylation deficiency leads to colitis and adenocarcinoma, loss of Notch activation, and downregulation of *Hes1*. HES1 loss correlates with development of human right-sided colorectal tumors with epigenetic loss of MLH1. These findings indicate that carcinogenesis in a subset of colon cancer is consequent to a molecular mechanism driven by fucosylation deficiency and/or HES1-loss.

Keywords

signal transduction; metabolism; tumorigenesis; colon cancer

Background

Fucosylation is an enzyme-catalyzed process that covalently links fucose (6-deoxy-L-galactose) to oligosaccharides and proteins. Fucosylation is regulated by fucosyltransferases, guanosine diphosphate (GDP)-fucose synthetic enzymes, and GDP-fucose transporters^{1, 2}. Fucosylated glycans are constructed by fucosyltransferases using the substrate GDP-fucose. Two GDP-fucose synthesis pathways exist in mammals. The GDP-mannose-dependent *de novo* pathway normally provides the majority of GDP-fucose synthetic capacity. A free fucose-dependent salvage pathway also exists, but normally contributes little if any to GDP-fucose synthetic capacity, unless intentionally supported by the administration of substantial amounts of exogenous free fucose. Conversion of GDP-mannose to GDP-fucose is accomplished by sequential reactions catalyzed by GDP-4,6-dehydratase (GMDS)³ and GDP-4-keto-6-deoxy-mannose-3,5-epimerase-4-reductase (FX)⁴. Fucosylation is an essential component of several blood group antigens, is implicated in host microbe interactions, and regulates cell adhesion molecules and growth factor receptors⁵⁻⁹. Fucosylation also enables fringe-dependent modulation of Notch signaling activation which leads to activation of downstream targets such as the *Hes* family genes^{10, 11}. Notch signaling in blood cells is regulated in part via Notch-Notch ligand interactions that involve *O*-fucosylation of multiple EGF-like repeats on the extracellular ligand binding domain of Notch receptors. This *O*-fucosylation is mediated by protein *O*-fucosyltransferase I (Pofut1), as well as by fringe-mediated extension of *O*-fucose¹²⁻¹⁶. In gut epithelium, Notch is essential for maintenance of intestinal proliferative crypt cells and control of secretory cell fate^{17, 18}. Multiple studies also find that Notch expression and/or signaling are dysregulated in colon cancer¹⁹, although there is not yet a clear understanding of the role of Notch in colon carcinogenesis.

Alterations in the expression of fucosylglycans have been observed in various cancers^{2, 20}. For example, increase in fucosylated alpha-fetoprotein is seen in sera of patients with hepatocellular carcinoma²¹. By comparison, loss of fucosylation due to mutation of *GMDS* is reported in colon cancer cell lines and up to 13% of colorectal cancer (CRC) tissues^{22, 23}. A search of the Cancer Genome Atlas (TCGA) reveals that homozygous deletions of *GMDS* are found in 2% of a published CRC database and in 5.5% of a provisional database²⁴ (www.cbioportal.org). However, it is not known if deficiency of fucosylation plays a determinant role in CRC development, or whether *GMDS* mutation correlates with or is causative of a pathogenic role for aberrant Notch signaling in colon carcinogenesis.

GMDS and FX mediate two sequential reactions in *de novo* GMD-fucose synthesis, allowing us to use mice with a deletion of the *Fx* locus²⁵ (referred as *Fx*^{-/-} mice hereafter) to explore a role for GDP-fucose-dependent mechanism in CRC pathogenesis. We reveal that without chemical or oncogenic induction, loss of fucosylglycan expression results in colonic inflammation, serrated-like lesions and frank adenocarcinoma, by implicating Notch dysregulation and downregulation of *Hes1*, while HES1 loss is also frequently found in human CRCs.

Results

Fx^{-/-} mice develop fucose-dependent inflammation, dysplasia, and colonic neoplasms

Deletion of *Fx* in mice disables *de novo* GDP-fucose synthesis. However, restoration of GDP-fucose generation can be achieved in these animals through the GDP-fucose salvage pathway via exogenous fucose supply^{15, 25}. *Fx*^{-/-} mice display weight-loss when maintained on a standard laboratory chow, but re-gain body weight when they are maintained on fucose-supplemented chow^{25, 26}. Here we extend these previous studies to evaluate progression of a colitis phenotype as a function of fucosylglycan depletion. To avoid a high mortality rate associated with new born mice maintained on standard chow, all new born mice were maintained on fucose-supplemented chow (hereafter referred to as on-fucose diet) until ~4 weeks of age. Mice were then maintained continuously with the on-fucose diet (equivalent to a wild type fucosylglycan phenotype), or were switched to standard chow (hereafter referred to as off-fucose diet, leading to a fucosylglycan-depleted phenotype) and maintained on that chow for up to 6 months. As expected, colon epithelium from mice maintained with the off-fucose diet (off-fucose mice) showed a loss of staining by Aleuria aurantia lectin (AAL), a lectin that recognizes $\alpha(1,3)/\alpha(1,4)$ and $\alpha(1,6)$ fucosylglycan configurations (Fig S1A). By contrast, epithelium from mice given the on-fucose diet (on-fucose mice) displayed robust AAL staining (Fig S1A) with normal histology (Fig 1A). Consistent with other reports, the intestines of off-fucose mice displayed goblet cell hyperplasia after transition to the off-fucose diet (data not shown)²⁶. In addition, in the off-fucose mice, we observed a diffuse intramural/submucosal inflammation restricted to the large intestine (Fig 1A), and sessile serrated adenoma-like lesions (SSLs) with architectural features of luminal dilation and horizontally branching growth (Fig S1B). These features were observed in off-fucose mice as early as 2 weeks after the switch to the off-fucose diet, but not in on-fucose mice. The inflammation was characterized by a thickened mucosa infiltrated by both acute and chronic inflammatory cells, crypt destruction and surface re-epithelization. Low-grade dysplasia appeared displaying hyperchromatic pseudostratified nuclei. As the duration of off-fucose diet increased, the low-grade dysplasia in some instances evolves into high-grade dysplasia, featuring increased nuclear polymorphism and architectural complexity (Fig S1C). Foci of dysplasia arising from SSLs were also observed (Fig S1B). These foci resemble those of human “sessile serrated adenoma (SSA) with cytological dysplasia”^{27, 28}. Colon inflammation was also evaluated by flexible colonoscopy, which disclosed mucosa bleeding, loss of mucosal transparency and focal lesions in off-fucose mice (Fig S2A). The severity of colitis, as gauged by inflammation scores (Fig 1C), and epithelial dysplasia (defined as the percentage of cells displaying dysplasia, Fig 1D), increased with the duration of the off-fucose diet. Notably, both colitis and dysplasia of *Fx*^{-/-} mice, as assessed by histology (Fig 1B-C) or colonoscopy (Fig S2A), were partially reversed 15 days after the off-fucose mice were switched back to the on-fucose diet, and these lesions were nearly completely reversed after 30 days of diet switch (Fig S2B). These findings imply that both inflammation and dysplasia of *Fx*^{-/-} mice colonic epithelium are strictly dependent on the fucosylation status of these mice.

Analysis of epithelia cytokine expression in the off-fucose mice was done using ELISA array. These analyses revealed an increased expression of pro-inflammatory cytokines,

including TNF α , IL-1 β , M-CSF, C5/C5a and sICAM-1 (not shown). This observation was corroborated by results of qRT-PCR analysis of mRNA extracted from the colonic epithelium of off-fucose mice showing a significant increase in expression of pro-inflammatory cytokine mRNAs, including TNF α , IL-1 β , IL-6, IL-17, IL-23, IFN γ , and Cox2, relative to cytokine mRNA expression in epithelium procured from on-fucose mice (Fig 1D). Cytokine mRNA expression was assessed throughout the remainder of the study because of the increased sensitivity of this method compared to the ELISA method. The increased expression of the cytokine mRNAs was largely reversed 30 days after off-fucose mice were switched back to on-fucose diet, supporting the conclusion that the epithelial inflammation of *Fx*^{-/-} mice is dependent on the fucosylation status of these mice.

Inflammation is associated with increased risk of developing colorectal cancer^{29,30}. Accordingly, adenocarcinomas were observed in off-fucose mice, as soon as one month after the mice were placed on off-fucose diet (Fig 1E). The incidence of adenocarcinoma increases as duration of off-fucose diet prolongs, reaching ~40% at 2-5 months after diet switch (Table S1). In contrast, none of the on-fucose mice developed CRC. Histologically, we observed neoplastic glands infiltrating through the muscularis mucosae throughout the whole length of colon, with the majority of the tumors (81%) found either in the proximal colon (Fig 1E) or in the cecum.

Altered colonic epithelial homeostasis associated with loss of Notch signaling in *Fx*^{-/-} mice

In concordance with a loss of Notch signal transactivation in the blood cells of *Fx*^{-/-} mice, as we described previously¹⁵, we observed that expression of activated Notch1 and Notch2, and the Notch target gene HES1 was decreased in the colon epithelium of off-fucose mice compared to on-fucose mice (Fig 2A). Consistent with the role of Notch in the regulation of progenitor proliferation^{17, 18}, in on-fucose mice, Ki67⁺ proliferating cells were abundant at the bottom of the crypts but were reduced or absent in epithelia cells moving towards to the top of the crypts, as observed in wild type mice (Fig 2B). By contrast, Ki67⁺ cells observed in off-fucose mice, where signaling by Notch1 and Notch2 is severely attenuated, display either a disorganized pattern mainly located in the middle or top of the crypts (off-fucose I'), or a diffuse distribution pattern in crypts displaying dysplastic features (off-fucose II') (Fig 2C). In addition, compared to on-fucose mice, off-fucose colonic epithelium had increased activation of NF- κ B and STAT3 (Fig S3A-B). This was accompanied by a progressive increase in gut epithelial permeability of off-fucose mice (Fig 2D) as a function of prolonged exposure to the off-fucose diet. Furthermore, disruption of the epithelial integrity in off-fucose mice was corrected 30 days after mice were switched back to the on-fucose diet (Fig 2D). These findings imply that the fucose-dependent gut epithelial pathology in *Fx*^{-/-} mice is consequent to loss of Notch activation, altered epithelial proliferation and impaired gut barrier function as a result of fucose deficiency.

Dependence of inflammation and dysplasia on gut microflora which displays compositional shift upon loss of epithelial fucosylation

The defective epithelial barrier function of fucose-deficient *Fx*^{-/-} mice in association with epithelial inflammation prompted us to examine the contribution of intestinal bacteria in

colitis and cancer development in *Fx*^{-/-} mice. We first asked whether epithelial fucosylation deficiency alters gut microflora. We performed 16s rRNA sequencing on fecal bacteria first collected from a group of *Fx*^{-/-} mice that were initially fed the on-fucose diet, then from the same mice at 2 and 4 weeks after switching diet to off-fucose, respectively, and again from these mice at 2 and 4 weeks after switching back to the on-fucose diet, respectively. Fecal bacteria collected from the WT mice fed with standard diet and then from the same mice after feeding on-fucose diet were also sequenced to control for a fucose-mediated direct effect on the gut microflora. We found that, at the class level of taxonomic ranking, fecal bacteria from all *Fx*^{-/-} mice displayed a distinct expansion in the abundance of *Verrucomicrobiae* compared to WT mice maintained with standard or on-fucose diet (Fig S4A). At the genus level, the expansion of *Verrucomicrobiae* class reflects an expansion of *Akkermansia* in all fecal DNA from *Fx*^{-/-} mice, and an even greater expansion in off-fucose mice. By comparison, although the overall proportion of *Bacteroidia* class was decreased in *Fx*^{-/-} mice compared to WT mice, the *Barnesiella* genus in this class showed an expansion only in fecal DNA from on-fucose *Fx*^{-/-} mice but not those from off-fucose *Fx*^{-/-} mice, and a trend towards an increase in those organisms from WT mice given the on-fucose diet. In addition, the proportion of the *Helicobacter* genus belonging to the *Epsilonproteobacteria* class in on-fucose *Fx*^{-/-} mice was decreased compared to the WT mice given on-fucose diet, and further decreased in off-fucose *Fx*^{-/-} mice (Fig 3A). Principle component analysis revealed a similar microflora population in WT mice fed with standard chow and those fed with on-fucose chow, whereas the microbial composition in *Fx*^{-/-} mice fed with off-fucose diet showed a significant shift relative to that in mice fed with on-fucose diet, with reversible change after switching back to on-fucose diet (Fig S4B). These observations imply that epithelial fucosylation deficiency is the major cause for the gut microbial shift in *Fx*^{-/-} mice, while fucose itself has a much more modest direct effect.

We then asked whether the gut microflora is required for the inflammation and dysplasia observed in *Fx*^{-/-} mice. Since the *Fx*^{-/-} and the WT mice used in this study were found to be colonized with *Helicobacter hepaticus* (*HH*) and 2 other *Helicobacter* species (data not shown), and *HH* is a known pathobiont implicated in several mouse models of colon cancer including C57BL/6 *IL10*^{-/-} mice and immune-compromised mice³¹⁻³³, we treated animals with antibiotic cocktails targeting a wide-spectrum of bacteria including the *Helicobacter* species. As expected, in treated mice, *HH* was not detected by PCR (Fig S5A). The overall fecal bacteria burden and the trans-luminal bacterial load, determined by 16s RT-PCR, was 2.3-fold and 1.8-fold higher, respectively, in off-fucose mice, relative to on-fucose mice. However, both were significantly decreased after antibiotic treatment (Fig 3B). Accordingly, colitis and dysplasia were improved in antibiotic-treated mice compared to non-treated mice (Fig 3C-D and Fig S5B). Furthermore, the increased epithelial permeability observed in off-fucose mice was nearly completely reversed after antibiotic treatment (Fig 3E), and none of the antibiotic-treated mice developed cancer (Table 1). By contrast, antibiotic treatment of on-fucose mice had no significant effect on colon epithelial histology (data not shown). These findings indicate that colitis and colon cancer in *Fx*^{-/-} mice was dependent on the gut microflora, which is in turn dependent upon the fucosylation status of the gut epithelium.

Fucose-deficient colonic epithelium is sufficient to cause inflammation and dysplasia

To determine the relative contribution to inflammation and cancer by the fucose-deficient epithelium and by the fucose-deficient hematopoietic cells, we performed reciprocal bone marrow transplantation in which WT or fucose-deficient marrow cells (Ly5.2) were transplanted into lethally-irradiated 8-week old wild type (WT; Ly5.1) or *Fx*^{-/-} mice (Ly5.1). *Fx*^{-/-} recipients were first fed on-fucose diet to decrease mortality associated with irradiation. At 10 days after receiving bone marrow transplantation, *Fx*^{-/-} recipients were switched to the off-fucose diet to allow *Fx*^{-/-} recipients and *Fx*^{-/-} donor cells to achieve fucosylation-deficient status in the epithelium as well as in blood cells. WT recipients received regular chow throughout the transplantation. Two months after diet switch following transplantation, mice were examined and scored for inflammation and dysplasia. Histological evaluation revealed that WT mice receiving WT or *Fx*^{-/-} bone marrow cells showed no inflammation nor epithelial dysplasia. By contrast, *Fx*^{-/-} mice receiving *Fx*^{-/-} marrow cells all became moribund at 4-6 weeks after transplantation, displaying more severe inflammation and dysplasia than *de novo* off-fucose mice (Fig 4A-B, Fig S6A). *Fx*^{-/-} recipients receiving WT marrow cells displayed modest colitis and dysplasia at 4 or 8 weeks after transplantation (Fig 4A-B; Fig S6B). The inflammation and dysplasia scores (7 and 18, respectively) at 8 weeks were improved when compared to off-fucose mice without transplantation (11 and 34, respectively) (Fig 4C-D; Table 1). These results indicate that *Fx*^{-/-} marrow cells did not autonomously cause inflammation and dysplasia, whereas *Fx*^{-/-} gut mucosa was sufficient to induce inflammation and dysplasia. However, inflammation and dysplasia was most severe in *Fx*^{-/-} host receiving *Fx*^{-/-} hematopoietic cells.

The milder colonic inflammation and dysplasia in *Fx*^{-/-} recipients receiving WT marrow cells could result from a phenotype rescue of the fucosylation-deficient epithelium by the WT cells, perhaps through fucose cross-feeding via catabolism of WT fucosylglycans by the *Fx*^{-/-} recipients. To examine this possibility, we stained the colon epithelium with AAL after transplantation. We found gut epithelium of *Fx*^{-/-} recipients receiving *Fx*^{-/-} marrow cells showed a loss of AAL staining, in contrast to a robust staining in WT recipients receiving WT or *Fx*^{-/-} marrow cells. By comparison, *Fx*^{-/-} recipients receiving WT marrow cells showed minimal AAL staining of colonic epithelium, but strong AAL reactivity in the inter-cryptic immune cells derived from the WT donors (Fig S6C). Thus, there appears to be a minimal re-gain of AAL reactivity in *Fx*^{-/-} epithelium after receiving WT marrow cells; however, the possibility of phenotype rescue remains possible because we found that inflammation and dysplasia further improved with average scores reaching 5 and 10, respectively, at 4 months, but did not completely convert to normal levels as observed in the *de novo* on-fucose mice (Fig 4C-D, Fig S6B).

The ability of the *Fx*^{-/-} gut mucosa to drive inflammation was further supported by findings of epithelial cytokine expression which showed that most cytokines except TNF α were not increased in WT hosts receiving *Fx*^{-/-} hematopoietic cells, but were increased in *Fx*^{-/-} host receiving WT marrow. Levels of IL-6 and TNF α were further increased in *Fx*^{-/-} host receiving *Fx*^{-/-} hematopoietic cells (Fig 4E). Furthermore, STAT3 and NF- κ B were not activated in WT mice receiving WT or *Fx*^{-/-} cells but were mildly increased in *Fx*^{-/-} recipients receiving WT marrow, and increased further in those receiving *Fx*^{-/-} marrow cells

(Fig S6D). These findings indicate that inflammation and pro-inflammatory cytokine expression were mainly driven by the fucose-deficient gut epithelium, while *Fx*^{-/-} hematopoietic cells may further enhance inflammatory response and dysplasia. Only one out of 12 *Fx*^{-/-} recipients receiving WT marrow cells developed adenocarcinoma, at 6 months after transplant (Table 1). By contrast, all *Fx*^{-/-} recipients receiving *Fx*^{-/-} hematopoietic cells died before they could be evaluated for CAC development.

Suppression of CD8 T cell cytotoxic function by fucose-deficient host

To begin to examine the mechanism underlying the dominant pro-inflammation and pro-dysplasia process driven by the fucosylation-deficient epithelium, we examined T cells isolated from the mesenteric lymph nodes (mLN) of on-fucose, off-fucose, and off-fucose *Fx*^{-/-} mice then switched back to on-fucose diet. We observed a mild alteration of CD4-expressing (data not shown) and CD8-expressing IFN γ (Fig 5A) but a striking reduction of Granzyme B (GzmB) expression by CD8 T cells in off-fucose mice compared to on-fucose mice, and a reversal of its expression in off-fucose mice switched back to on-fucose diet (Fig 5B). We then examined donor-derived (Ly5.2) mLN T cells, either from WT or *Fx*^{-/-} donors, arising after bone marrow transplantation in WT or *Fx*^{-/-} recipients, respectively. We found that, upon *ex vivo* stimulation, CD8 IFN γ levels showed a moderate increase in *Fx*^{-/-} T cells reconstituted in WT mice (Fig 5C). By comparison, GzmB production by CD8 T cells was decreased by ~50% in both WT and *Fx*^{-/-} donor cells that reconstituted *Fx*^{-/-} hosts (Fig 5D), when compared to those made by CD8 counterparts reconstituting WT recipients. These findings suggest that CD8 T cell cytotoxic effectors were prominently inhibited in fucose-deficient hosts.

Loss of HES1 expression is frequently found in right-sided colon cancer

Finally, we evaluated the relevance of fucosylation-deficiency and Notch dysregulation in human CRC. We found that 10 of the 11 *GMDS*-deleted cases reported by TCGA are right-sided or involve transverse colon.²⁴ This observation is similar to the observation in *Fx*^{-/-} mice, where a majority of the tumors in these animals are found either in the cecum or in the proximal colon. We recently reported that >90% of human SSAs have lost nuclear HES1 expression³⁴. Since SSAs mainly affect the right side and transverse colon, we asked whether loss of HES1 is also a feature of right-sided CRC. We examined a panel of 60 archived human CRC specimens (27 left-sided, 33 right-sided). Overall, HES1 reactivity can be classified into three groups: positive, with consistent nuclear staining in epithelial cells and crypt cells (Fig 6A); negative, with no or very weak nuclear staining of epithelial and crypt cells but positive staining in the lamina propria immune cells (Fig 6B); and heterogeneous, with mixed reactivity in only a portion of the nuclei (Fig 6C)³⁴. A few cases showing cytoplasmic HES1 staining with weak peri-nuclei or negative nuclear reactivity were classified in the negative group because of the lack of HES1 transcriptional activity. We found that 85% (28/33) of right-sided CRCs show complete loss of HES1, whereas HES1 loss is less common in the left-sided colon cancer (7/27, 26%). Uniformly increased nuclear expression of HES1 in invasive carcinoma is mostly seen in left (14/27, 52%) and rarely seen in right colon (3/33, 9%). Heterogeneous immunostaining is present in a subgroup of right (2/33, 6%) and left colon cancer (6/27, 22%). In addition, 80% of HES1 (-) CRCs have lost expression of MLH1 (one of several DNA mismatch repair proteins) due

to promoter methylation, whereas only 8% of HES1 (+) CRCs have epigenetic loss of MLH1. Therefore, there is significant correlation of HES1 loss with right side location of the tumor ($r=0.63$, $p<0.001$) or with MLH1 epigenetic loss ($r=0.67$, $p<0.001$).

Discussion

In this study, we examined a mouse model of colon cancer in the setting of fucosylation deficiency (*Fx*^{-/-} mice), a biochemical defect also caused by *GMDS* deletion and mutation seen in human CRC²²⁻²⁴. We find that fucose-deficient epithelium displays suppressed Notch activation and decreased expression of Notch target *Hes1*. Consistent with Notch being essential for the maintenance of intestinal epithelial homeostasis^{19, 20}, *Fx*^{-/-} mice colonic epithelium is characterized by goblet cell expansion and aberrant crypt proliferation. In addition, we observe that fucose-deficient epithelium plays a dominant role in inducing inflammation and tumorigenesis by affecting gut mucosal integrity and by influencing gut microflora. Furthermore, we observe that fucose-deficient epithelium plays a critical role in modulating immune response by suppressing T cell Gzm B expression. Lastly, following our previous reports of HES1 loss in human SSA³⁴, we find that HES1 loss is seen in the majority of human right-sided colon cancers displaying epigenetic loss of MLH1, supporting a potential pathogenic role of HES1 loss in human colon cancer development.

In this carcinogen-free colon cancer model, *Fx*^{-/-} mice develop colitis, dysplasia and adenocarcinoma in a defined temporal and histopathological sequence. Inflammation is likely a major pathogenic factor to cause carcinogenesis in *Fx*^{-/-} mice, as dysplasia and cancer is prevented when inflammation is controlled by antibiotics, even though the epithelium remains fucose-deficient. Notably, colitis in *Fx*^{-/-} mice is interwoven with lesions carrying architectural features of human SSA. While patients with inflammatory bowel disease (IBD) are at increased risk of developing dysplasia and colorectal cancer^{29,30}, there is also emerging evidence that serrated adenomas are found in IBD patients and may contribute to colon cancer development³⁵. However, neither is the contribution of SSL to the tumorigenesis in this animal model well understood, nor are the natural history and the clinicopathologic features of human IBD-associated serrated lesions clearly defined. Mixed types of inflammatory cytokines are increased in the inflamed epithelium of the *Fx*^{-/-} mice accompanied with increased Ki67 proliferative index. Likewise, inflammatory cytokines such as Cox2, IL-1 β , TNF α are increased in human serrated adenomas^{36, 37}. These findings suggest that colitis-associated serrated lesions are likely reflective of aberrant proliferation associated with inflammation as observed in the *Fx*^{-/-} mice and in other animal models³⁸. These colitis-associated serrated lesions may be associated with an altered immune microenvironment and the microflora dysbiosis induced by fucosylation deficiency in the *Fx*^{-/-} mice, and likewise, associated with alterations in the microbiota and immune response related to specific genetic factor in human IBD-associated neoplasia³⁹. Future studies are needed to define if SSLs of *Fx*^{-/-} mice carry the molecular hallmarks of human serrated neoplasia, and are consequent to defective Notch/HES1 signaling (see below). We speculate findings from the *Fx*^{-/-} mice could be applied to better understand the clinicopathophysiology of IBD-related neoplasia³⁹.

Consistent with our findings in the hematopoietic system that fucosylation deficiency disables Notch signaling, expression of activated Notch receptors and Notch target *Hes1* in *Fx*^{-/-} mice gut epithelium is severely diminished. However, a causal role of *Hes1* loss in the carcinogenesis has yet to be established. *Hes1* knockout mice have secretory cell expansion⁴⁰, sharing some intestinal pathologic features with *Fx*^{-/-} mice. However, *Hes1* knockout mice do not develop serrated lesion or colon cancer, presumably because *Hes1* functional loss was compensated for by other family members⁴¹, a compensation that would not be possible in the *Fx*^{-/-} mice. Nevertheless, our animal findings support an inflammation- and tumor-suppressive function of Notch/HES1 in colon epithelium during CRC development. We previously found a strong association of HES1 loss with SSA³⁴, a precursor lesion for CRC, and with CRCs displaying MLH-1 epigenetic loss in this study. The majority of SSAs show a homogenous loss of nuclear HES1 expression compared to the normal colon and the hyperplastic polyps where nuclear HES1 expression indicate normal HES1 function as a transcription factor. A few cases of SSAs with cytologic dysplasia show a diffuse cytoplasmic HES1 reactivity with weak peri-nuclei staining or negative nuclear reactivity, suggestive of altered HES1 distribution but continued HES1 dysregulation³⁴. This pattern of cytoplasmic HES1 reactivity was also found in some CRCs; however, its clinical significance would be best defined with longitudinal follow-up of the clinical course of SSA transition to SSA with dysplasia and to carcinoma development in the serrated colon cancer pathway. We speculate that cytoplasmic HES1 expression may be caused by an altered HES1 transport or degradation mechanism, or related to genetic and/or epigenetic changes that are necessary for the transition to SSA with dysplasia but not necessarily required for the carcinoma development. Additional work is needed to elucidate the cellular and the molecular mechanism that mediates HES1 loss in SSA and CRC. While *GMD5*-mutated CRC shows HES1 loss as expected (Fig S7), HES1-negative tumors are not necessarily to be related to fucosylation deficiency, because *GMD5* mutation/deletion is relatively rare compared to HES1 loss in human CRC. Finally, a few IBD-related serrated lesions (Fig S7A) and IBD-associated CRCs we examined including one *GMD5*-mutated case (Fig S7B) show loss of nuclear HES1 expression; however, the contribution of HES1 loss to the development and the clinicopathophysiology of IBD-associated neoplasia requires further investigation in a large human tissue cohort.

Fucosylglycans decorate proteins and lipids throughout the mammalian gastrointestinal tract and play an important role in host-microbe symbiosis⁴². Recent findings revealed that commensal bacteria mediate the expression of IL-22 by innate lymphoid cells which in turn stimulate $\alpha(1,2)$ fucosyltransferase (Fut2)⁴³, and individuals lacking a functional copy of *FUT2* display significant differences in their gut microbiome community structure⁴⁴. Here we report that colon mucosa is also decorated by fucosylglycan chains in $\alpha(1,3)$ and $\alpha(1,6)$ configurations recognized by AAL. Functions for these fucosylglycans and *O*-fucosylated glycans in gastrointestinal diseases have not been addressed¹. *GMD5* deleted/mutated CRCs and their phenotype-matched animals offer opportunities to investigate a broader role of fucosylation in human diseases including CRC. Interestingly, our work reveals that a general depletion of epithelial fucosylation affects the gut microbiome structure with expansion or reduction of certain bacterial subsets. Whether any of these bacteria species has a pathogenic role in inflammation and neoplastic transformation remains to be determined. It will be

interesting to investigate if fucose-deficiency caused by *GMDS* deletion/mutation in human also induces microflora dysbiosis and inflammation that compromise mucosal barrier function. Importantly, we observe that fucosylglycan restoration in gut mucosa restored compromised gut permeability, and led to decreased bacterial invasion, supporting a critical requirement for an intact epithelium with fucosylation modification in protecting mice against colitis and carcinogenesis. These observations indicate that fucose-supplementation may be an effective therapeutic approach in protecting mucosa homeostasis and in preventing inflammation and carcinogenic transformation in patients who have compromised mucosal barrier function caused by fucosylglycan deficiency due to *GMDS* deletion/mutation or other defects in fucosylglycan biosynthesis.

In bone marrow transfer experiments, we reveal that epithelial inflammation of *Fx*^{-/-} mice featured a mixed type of cytokine effectors that were predominantly driven by the fucose-deficient host. Analysis of mesenteric lymph node T cells in *Fx*^{-/-} mice maintained with off-fucose diet reveal a significant suppression of CD8 T cell Gzm B production. Furthermore, after WT bone marrow cells reconstitute lethally-irradiated *Fx*^{-/-} mice, the developing T cells derived from normal donors also display a suppression of T cytotoxic function. These observations suggest that the immune defects associated with the gut pathology are primarily determined by the host factors in fucosylation-deficient mice, but not the fucosylation-deficient blood cells. However, the exact mechanism underlying this fucosylation deficiency-driven immune suppression remains to be determined.

In summary, *Fx*^{-/-} mice is an excellent animal model to study the mechanism and the pathophysiology of human CRCs that carry genetic mutations/deletions affecting fucose metabolism, and cancers that display loss of Notch/HES1 signaling, dependent or independent of fucose deficiency.

Materials and methods

Mice and bone marrow transplantation

The animal research related to this article was approved by Case Western Reserve University Institutional Animal Care and Use Committee. *Fx*^{-/-} mice were maintained and prepared as described^{15, 25}. In some experiments, we treated 8- to 12-wk-old *Fx*^{-/-} mice under conventional conditions, or 2 weeks after mice receiving bone marrow transplantation, with medicated feed *ad lib* containing amoxicillin (0.06%), clarithromycin (0.01%), metronidazole (0.02%) and omeprazole (0.0004%) for 8 wks⁴⁵. Bone marrow transplantation was performed in lethally-irradiated mice (Ly5.1) by i.v. transfer of 2×10^6 donor cells (Ly5.2)¹⁵.

Epithelial permeability analysis

Colon permeability assay was performed using FITC-dextran. In brief, mice were fasted for 4h followed by rectal administration of 4 kDa FITC-dextran (1 mg/g body weight). Plasma was collected 1hr later. Serum fluorescence intensity was measured using a microplate analyzer (PerkinElmer VICTOR3) and concentrations were calculated from a standard curve of FITC-dextran serial dilution.

Human tissue collection and IHC

Study of archived human CRC was approved by the Institutional Research Board (IRB) of the University Hospitals Case Medical Center. Please see details in Supplemental Information.

Other Methods

For histology, western blot, immunohistochemistry, AAL staining, 16s RNA sequencing, mouse colonoscopy, T cell stimulation, flow analysis, and qRT-PCR, please see details in Supplemental Information.

Supplementary Material

Refer to Web version on PubMed Central for supplementary material.

Acknowledgments

Funding: Part of the work was supported by grants from American Cancer Society LIB-125064 and NIH HL103827 to L.Z., by the histology/imaging core support from the Cleveland Digestive Disease Research Core Center (CDDRCC) P30DK097948 to F.C., and by Department of Pathology Case Western Reserve University faculty startup fund to W. X. and L. Z.

References

1. Becker DJ, Lowe JB. Fucose: biosynthesis and biological function in mammals. *Glycobiology*. 2003; 13:41R–53R.
2. Miyoshi E, Moriwaki K, Nakagawa T. Biological function of fucosylation in cancer biology. *J Biochem*. 2008; 143:725–9. [PubMed: 18218651]
3. Tonetti M, Sturla L, Bisso A, et al. Synthesis of GDP-L-fucose by the human FX protein. *J Biol Chem*. 1996; 271:27274–9. [PubMed: 8910301]
4. Ohyama C, Smith PL, Angata K, et al. Molecular cloning and expression of GDP-D-mannose-4,6-dehydratase, a key enzyme for fucose metabolism defective in Lec13 cells. *J Biol Chem*. 1998; 273:14582–7. [PubMed: 9603974]
5. Larsen RD, Ernst LK, Nair RP, et al. Molecular cloning, sequence, and expression of a human GDP-L-fucose:beta-D-galactoside 2-alpha-L-fucosyltransferase cDNA that can form the H blood group antigen. *Proc Natl Acad Sci U S A*. 1990; 87:6674–8. [PubMed: 2118655]
6. Kelly RJ, Ernst LK, Larsen RD, et al. Molecular basis for H blood group deficiency in Bombay (Oh) and para-Bombay individuals. *Proc Natl Acad Sci U S A*. 1994; 91:5843–7. [PubMed: 7912436]
7. Lowe JB. Selectin ligands, leukocyte trafficking, and fucosyltransferase genes. *Kidney Int*. 1997; 51:1418–26. [PubMed: 9150453]
8. Hooper LV, Gordon JI. Glycans as legislators of host-microbial interactions: spanning the spectrum from symbiosis to pathogenicity. *Glycobiology*. 2001; 11:1R–10R. [PubMed: 11181556]
9. Wang Y, Shao L, Shi S, et al. Modification of epidermal growth factor-like repeats with O-fucose. Molecular cloning and expression of a novel GDP-fucose protein O-fucosyltransferase. *J Biol Chem*. 2001; 276:40338–45. [PubMed: 11524432]
10. De Strooper B, Annaert W, Cupers P, et al. A presenilin-1-dependent gamma-secretase-like protease mediates release of Notch intracellular domain. *Nature*. 1999; 398:518–22. [PubMed: 10206645]
11. Jeffries S, Robbins DJ, Capobianco AJ. Characterization of a high-molecular-weight Notch complex in the nucleus of Notch(ic)-transformed RKE cells and in a human T-cell leukemia cell line. *Mol Cell Biol*. 2002; 22:3927–41. [PubMed: 11997524]
12. Koch U, Lacombe TA, Holland D, et al. Subversion of the T/B lineage decision in the thymus by lunatic fringe-mediated inhibition of Notch-1. *Immunity*. 2001; 15:225–36. [PubMed: 11520458]

13. Visan I, Tan JB, Yuan JS, et al. Regulation of T lymphopoiesis by Notch1 and Lunatic fringe-mediated competition for intrathymic niches. *Nat Immunol.* 2006; 7:634–43. [PubMed: 16699526]
14. Lu L, Stanley P. Roles of O-fucose glycans in notch signaling revealed by mutant mice. *Methods Enzymol.* 2006; 417:127–36. [PubMed: 17132502]
15. Zhou L, Li LW, Yan Q, et al. Notch-dependent control of myelopoiesis is regulated by fucosylation. *Blood.* 2008; 112:308–19. [PubMed: 18359890]
16. Yao D, Huang Y, Huang X, et al. Protein O-fucosyltransferase 1 (Pofut1) regulates lymphoid and myeloid homeostasis through modulation of Notch receptor ligand interactions. *Blood.* 2011; 117:5652–62. [PubMed: 21464368]
17. van Es JH, van Gijn ME, Riccio O, et al. Notch/gamma-secretase inhibition turns proliferative cells in intestinal crypts and adenomas into goblet cells. *Nature.* 2005; 435:959–63. [PubMed: 15959515]
18. Fre S, Huyghe M, Mourikis P, et al. Notch signals control the fate of immature progenitor cells in the intestine. *Nature.* 2005; 435:964–8. [PubMed: 15959516]
19. Qiao L, Wong BC. Role of Notch signaling in colorectal cancer. *Carcinogenesis.* 2009; 30:1979–86. [PubMed: 19793799]
20. Moriwaki K, Miyoshi E. Fucosylation and gastrointestinal cancer. *World J Hepatol.* 2010; 2:151–61. [PubMed: 21160988]
21. Aoyagi Y, Isemura M, Suzuki Y, et al. Fucosylated alpha-fetoprotein as marker of early hepatocellular carcinoma. *Lancet.* 1985; 2:1353–4.
22. Moriwaki K, Noda K, Furukawa Y, et al. Deficiency of GMDS leads to escape from NK cell-mediated tumor surveillance through modulation of TRAIL signaling. *Gastroenterology.* 2009; 137:188–98. 198 e1–2. [PubMed: 19361506]
23. Nakayama K, Moriwaki K, Imai T, et al. Mutation of GDP-mannose-4,6-dehydratase in colorectal cancer metastasis. *PLoS One.* 2013; 8:e70298. [PubMed: 23922970]
24. Comprehensive molecular characterization of human colon and rectal cancer. *Nature.* 2012; 487:330–7. [PubMed: 22810696]
25. Smith PL, Myers JT, Rogers CE, et al. Conditional control of selectin ligand expression and global fucosylation events in mice with a targeted mutation at the FX locus. *J Cell Biol.* 2002; 158:801–15. [PubMed: 12186857]
26. Waterhouse CC, Johnson S, Phillipson M, et al. Secretory cell hyperplasia and defects in Notch activity in a mouse model of leukocyte adhesion deficiency type II. *Gastroenterology.* 2010; 138:1079–90 e1–5. [PubMed: 19900444]
27. Rex DK, Ahnen DJ, Baron JA, et al. Serrated lesions of the colorectum: review and recommendations from an expert panel. *Am J Gastroenterol.* 2012; 107:1315–29. quiz 1314, 1330. [PubMed: 22710576]
28. Batts KP. The pathology of serrated colorectal neoplasia: practical answers for common questions. *Mod Pathol.* 2015; 28(1):S80–7. [PubMed: 25560602]
29. Eaden JA, Abrams KR, Mayberry JF. The risk of colorectal cancer in ulcerative colitis: a meta-analysis. *Gut.* 2001; 48:526–35. [PubMed: 11247898]
30. Beaugerie L, Svrcek M, Seksik P, et al. Risk of colorectal high-grade dysplasia and cancer in a prospective observational cohort of patients with inflammatory bowel disease. *Gastroenterology.* 2013; 145:166–175e8. [PubMed: 23541909]
31. Berg DJ, Davidson N, Kuhn R, et al. Enterocolitis and colon cancer in interleukin-10-deficient mice are associated with aberrant cytokine production and CD4(+) TH1-like responses. *J Clin Invest.* 1996; 98:1010–20. [PubMed: 8770874]
32. Ward JM, Anver MR, Haines DC, et al. Inflammatory large bowel disease in immunodeficient mice naturally infected with *Helicobacter hepaticus*. *Lab Anim Sci.* 1996; 46:15–20. [PubMed: 8699813]
33. Foltz CJ, Fox JG, Cahill R, et al. Spontaneous inflammatory bowel disease in multiple mutant mouse lines: association with colonization by *Helicobacter hepaticus*. *Helicobacter.* 1998; 3:69–78. [PubMed: 9631303]
34. Cui M, Awadallah A, Liu W, et al. Loss of Hes1 Differentiates Sessile Serrated Adenoma/Polyp From Hyperplastic Polyp. *Am J Surg Pathol.* 2016; 40:113–9. [PubMed: 26448192]

35. Iacucci M, Hassan C, Fort Gasia M, et al. Serrated adenoma prevalence in inflammatory bowel disease surveillance colonoscopy, and characteristics revealed by chromoendoscopy and virtual chromoendoscopy. *Can J Gastroenterol Hepatol*. 2014; 28:589–94. [PubMed: 25575106]
36. Szyllberg L, Janiczek M, Popiel A, et al. Expression of COX-2, IL-1beta, TNF-alpha and IL-4 in epithelium of serrated adenoma, adenoma and hyperplastic polyp. *Arch Med Sci*. 2016; 12:172–8. [PubMed: 26925134]
37. Kiedrowski M, Mroz A, Kraszewska E, et al. Cyclooxygenase-2 immunohistochemical expression in serrated polyps of the colon. *Contemp Oncol (Pozn)*. 2014; 18:409–13. [PubMed: 25784839]
38. Bongers G, Pacer ME, Geraldino TH, et al. Interplay of host microbiota, genetic perturbations, and inflammation promotes local development of intestinal neoplasms in mice. *J Exp Med*. 2014; 211:457–72. [PubMed: 24590763]
39. Matkowskyj KA, Chen ZE, Rao MS, et al. Dysplastic lesions in inflammatory bowel disease: molecular pathogenesis to morphology. *Arch Pathol Lab Med*. 2013; 137:338–50. [PubMed: 23451745]
40. Jensen J, Pedersen EE, Galante P, et al. Control of endodermal endocrine development by Hes-1. *Nat Genet*. 2000; 24:36–44. [PubMed: 10615124]
41. Ueo T, Imayoshi I, Kobayashi T, et al. The role of Hes genes in intestinal development, homeostasis and tumor formation. *Development*. 2012; 139:1071–82. [PubMed: 22318232]
42. Pickard JM, Chervonsky AV. Intestinal fucose as a mediator of host-microbe symbiosis. *J Immunol*. 2015; 194:5588–93. [PubMed: 26048966]
43. Goto Y, Obata T, Kunisawa J, et al. Innate lymphoid cells regulate intestinal epithelial cell glycosylation. *Science*. 2014; 345:1254009. [PubMed: 25214634]
44. Rausch P, Rehman A, Kunzel S, et al. Colonic mucosa-associated microbiota is influenced by an interaction of Crohn disease and FUT2 (Secretor) genotype. *Proc Natl Acad Sci U S A*. 2011; 108:19030–5. [PubMed: 22068912]
45. Kostomitsopoulos N, Donnelly H, Kostavasili I, et al. Eradication of *Helicobacter bilis* and *H. hepaticus* from infected mice by using a medicated diet. *Lab Anim (NY)*. 2007; 36:37–40. [PubMed: 17450169]

Abbreviations

GDP	guanosine diphosphate
GMDS	GDP-mannose 4,6-dehydratase
FX	GDP-4-keto-6-deoxymannose 3,5-epimerase-4-reductase
CRC	colorectal cancer
AAL	aleuria aurantia lectin
SSA	sessile serrated adenoma
SSL	serrated-like lesion
qRT-PCR	quantitative reverse transcription polymerase chain reaction
TCGA	the Cancer Genome Atlas
MSI	microsatellite instability
mLN	mesenteric lymph node

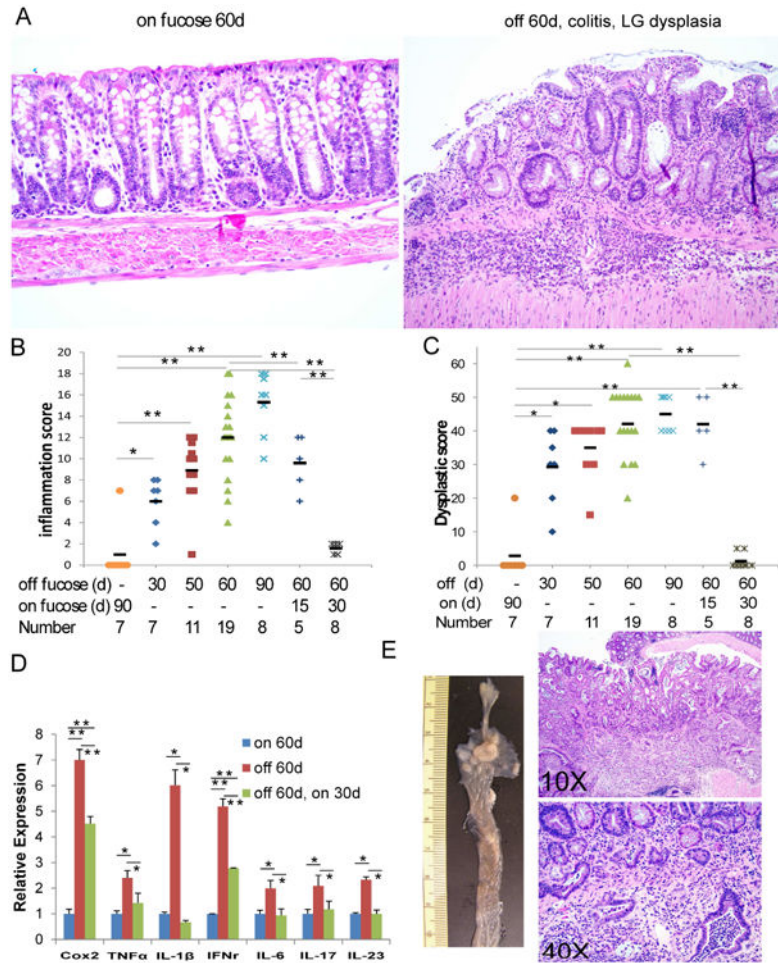


Fig 1. *Fx*^{-/-} mice develop fucose deficiency-dependent colitis and dysplasia with progression to adenocarcinoma

(A) Representative H&E staining shows normal colon tissue from *Fx*^{-/-} mice fed on-fucose diet for 60d, colon from *Fx*^{-/-} mice fed off-fucose diet for 60d showing colitis. Images were taken under 40 \times magnification. Scores of inflammation (B) and dysplasia (C) were measured in colon tissues from mice receiving on-fucose diet 90d, off-fucose for varying days, and those having off-fucose diet followed by on-fucose diet for 15d or 30d, respectively. Data was pooled from 3 experiments. Black bars indicate mean values. (D) Expression of inflammatory cytokines in colon epithelium was measured by qRT-PCR and normalized to those in on-fucose mice (n=5 from 2 experiments). Data shown represent mean \pm SD. (E) A representative gross histology and H&E staining (10 \times and 40 \times magnification) of adenocarcinoma in the proximal colon. Student *t*-test was performed for analysis in B, C and D. * p <0.05, ** p <0.01

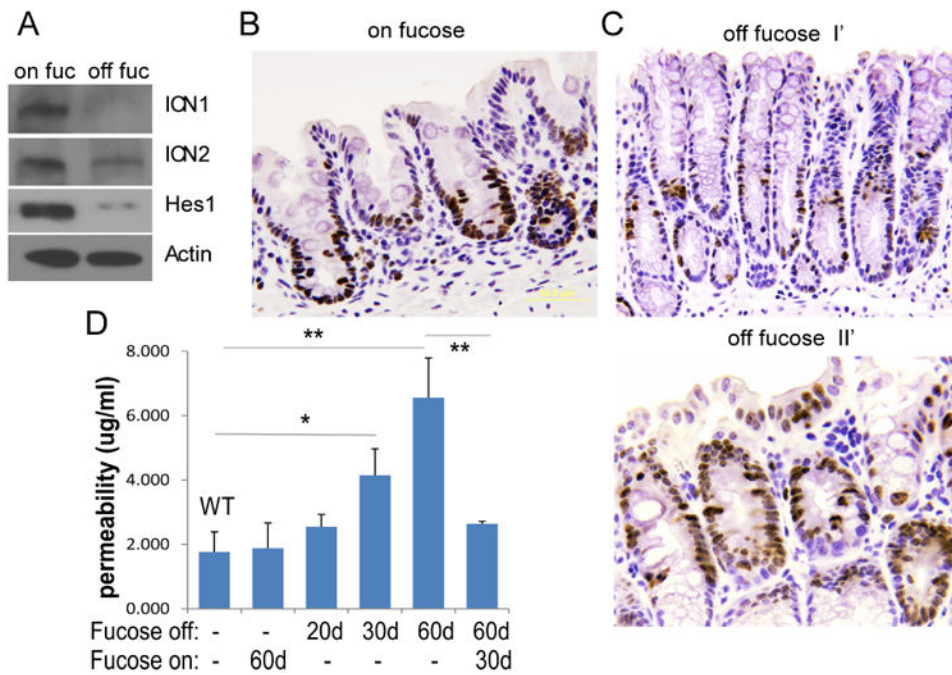


Fig 2. Altered colonic epithelial homeostasis associated with loss of Notch signaling in *Fx*^{-/-} mice (A) A representative western blot of colon epithelial protein extracts from *Fx*^{-/-} mice, either fed on-fucose (on fuc) or off-fucose diet (off fuc) for 60d, with antibodies against cleaved Notch1 (ICN1), Notch2 (ICN2), HES1, and β -actin. (B-C) Representative IHC staining of proliferating crypts with anti-Ki67 in colon of on-fucose mice (40 \times) (B), off-fucose mice (I': 20 \times ; II': 40 \times) (C). (D) Epithelial permeability was measured in WT, on-fucose (60d), and off-fucose mice for varying period of time, and off-fucose mice (60d) followed by on-fucose diet for 30d (n=5-9 in each group, from 3 experiments). Data shown in D represent mean \pm SD. Student *t*-test was performed. **p*<0.05, ***p*<0.01

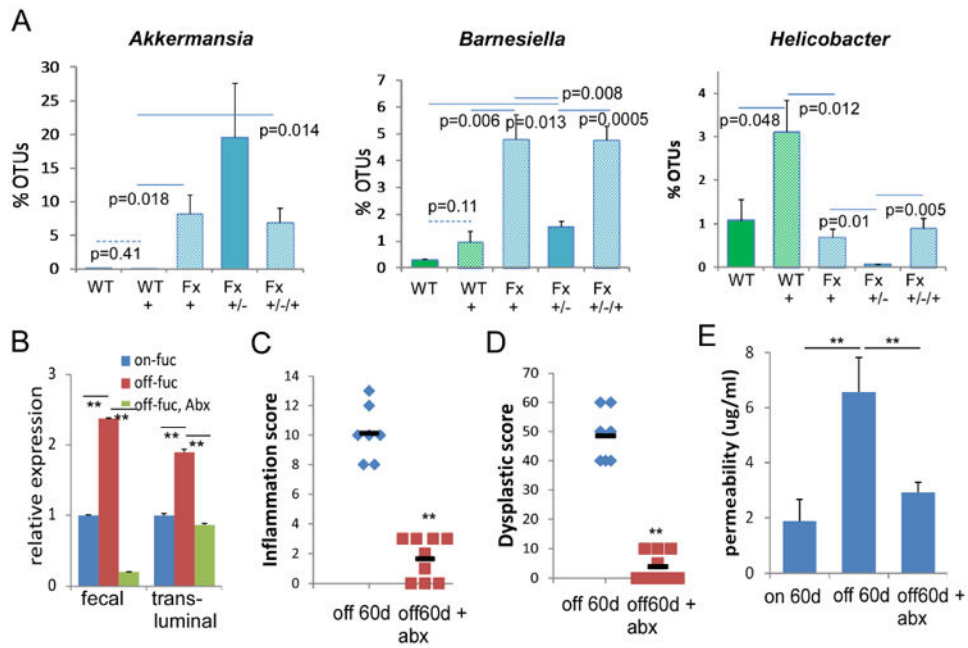


Fig 3. Microflora analysis and the requirement of gut microflora in *Fx*^{-/-} mice colon pathology (A) Fecal bacterial DNA was prepared from 5 WT mice maintained with regular diet (WT), from the same group of mice after feeding on-fucose diet 4wks (WT+), and from 5 *Fx*^{-/-} mice, first collected after feeding on-fucose diet 4wks (*Fx*+), second after 4 wks of switching to off-fucose diet (*Fx*+/-), and third collection after 4 wks of switching back to on-fucose diet (*Fx*+/-/+). Relative genus abundance was shown as percentage of each OTU in the total OTUs. Data shown represent means±SD (n=5/group). (B) Fecal bacteria and colon trans-luminal tissue bacteria burden were determined by qRT-PCR of 16s rRNA from on-fucose (60d) (on-fuc), off-fucose mice (60d) (off-fuc), and off-fucose mice treated with antibiotics (60d) (off-fuc, Abx). Data are expressed as the fold of change relative to that from on-fucose mice (n=4-5/group from 2 experiments). (C-E) Colon inflammation (C) and dysplasia scores (D), and epithelial permeability (E) were recorded for *Fx*^{-/-} mice fed off-fucose diet 60d and mice fed off-fucose diet plus antibiotics (n=6/group from 3 experiments). Data shown in A-E represent means±SD. Student *t*-test was performed; **p*<0.05, ***p*<0.01

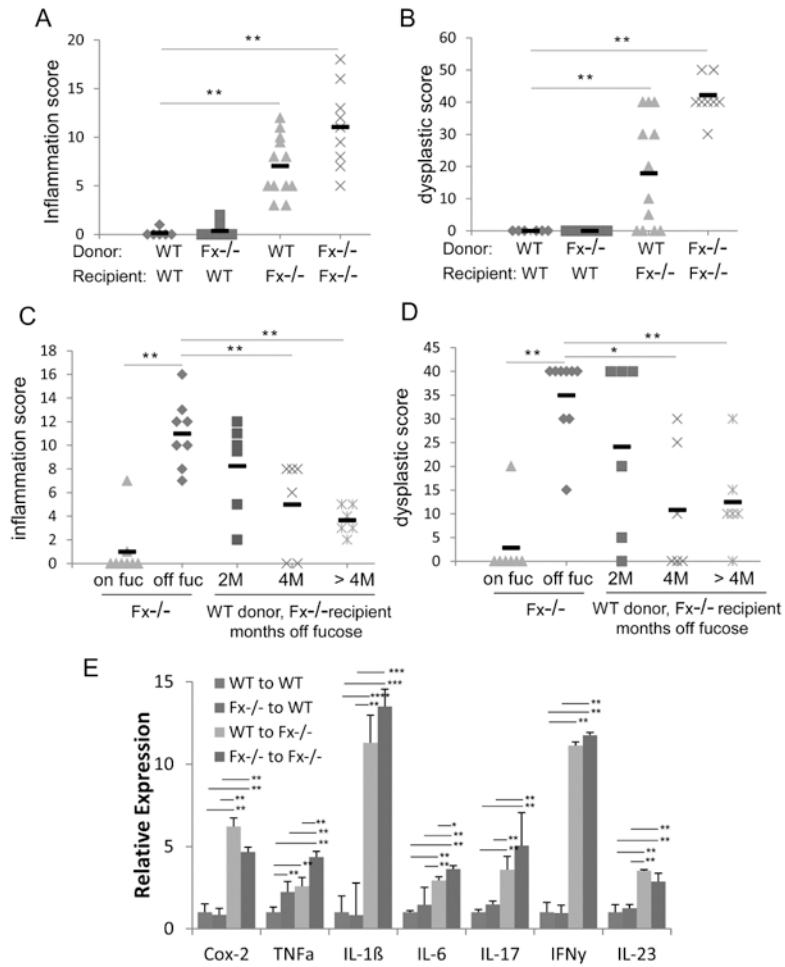


Fig 4. Fucosylation-deficient epithelium drives inflammation and dysplasia

Reciprocal transplantation was performed in WT mice receiving WT (n=6) or *Fx*^{-/-} marrow (n=8), in *Fx*^{-/-} mice receiving WT (n=12) or *Fx*^{-/-} marrow cells (n=9). Data were pooled from 4 experiments. Colon inflammation (A) and dysplastic scores (B) were recorded 2 months after transplantation. (C-D) In the setting of *Fx*^{-/-} mice receiving WT cells, colon inflammation (C) and dysplastic scores (D) were determined from colon tissues at 2 months (n=6), 4 months (n=6), and up to 6 months (>4 months; n=6) after transplantation, and compared to those of *Fx*^{-/-} mice fed on-fucose (on fuc; n=7) or off-fucose diet (off fuc; n=9). Data were pooled from 2 experiments. (E) Inflammatory cytokine mRNA expression in colon tissue from recipients in 4 transplant settings was measured by qRT-PCR and normalized to the expression in WT mice receiving WT cells (n=6-9/group from 3 experiments). Black bars in A-D indicate means. Results shown in E were mean±SD. Student *t*-test was performed; **p*<0.05, ***p*<0.01

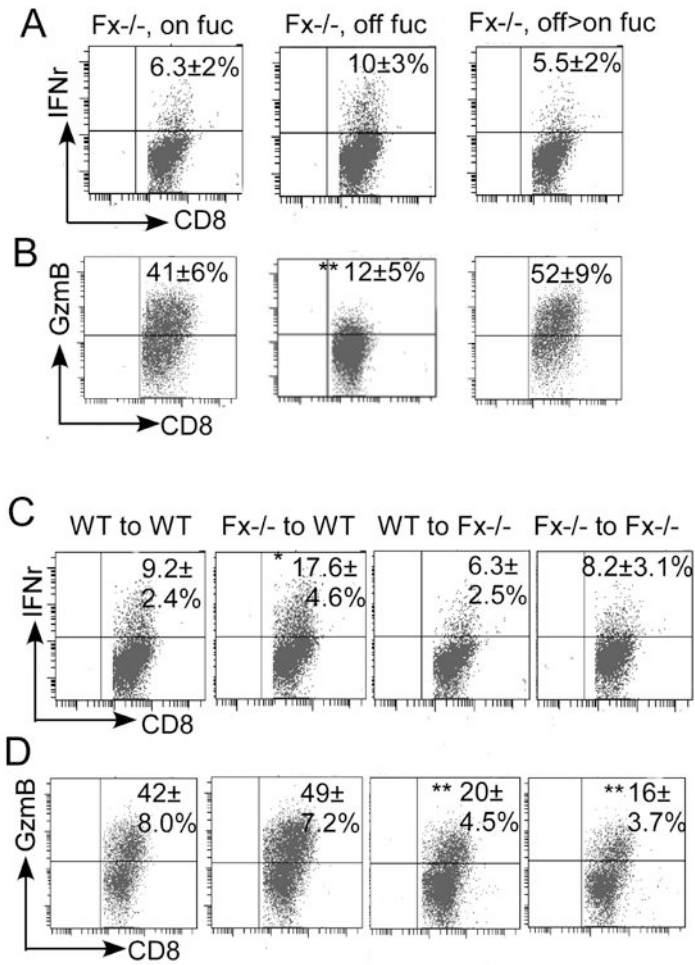


Fig 5. Host-driven suppression of CD8 T effector expression in *Fx*^{-/-} mice

(A-B) T cells of mLN were collected from on-fucose, off-fucose, and off-fucose *Fx*^{-/-} mice switched back to on-fucose diet. Intracellular staining for CD8 T cell IFN γ (A) and Granzyme B (B) were shown after anti-CD3/CD28 re-stimulation. (C-D) Representative flow plots of T cell analysis collected from WT or *Fx*^{-/-} mice receiving WT or *Fx*^{-/-} cells. Intracellular staining for IFN γ (C) and Granzyme B (D) were shown in Ly5.2⁺ CD8 T cells. Numbers indicate mean \pm SD (% of CD8⁺ cells; n=3-5/group from 2 experiments). Student *t*-test was performed; **p*<0.05, ***p*<0.01

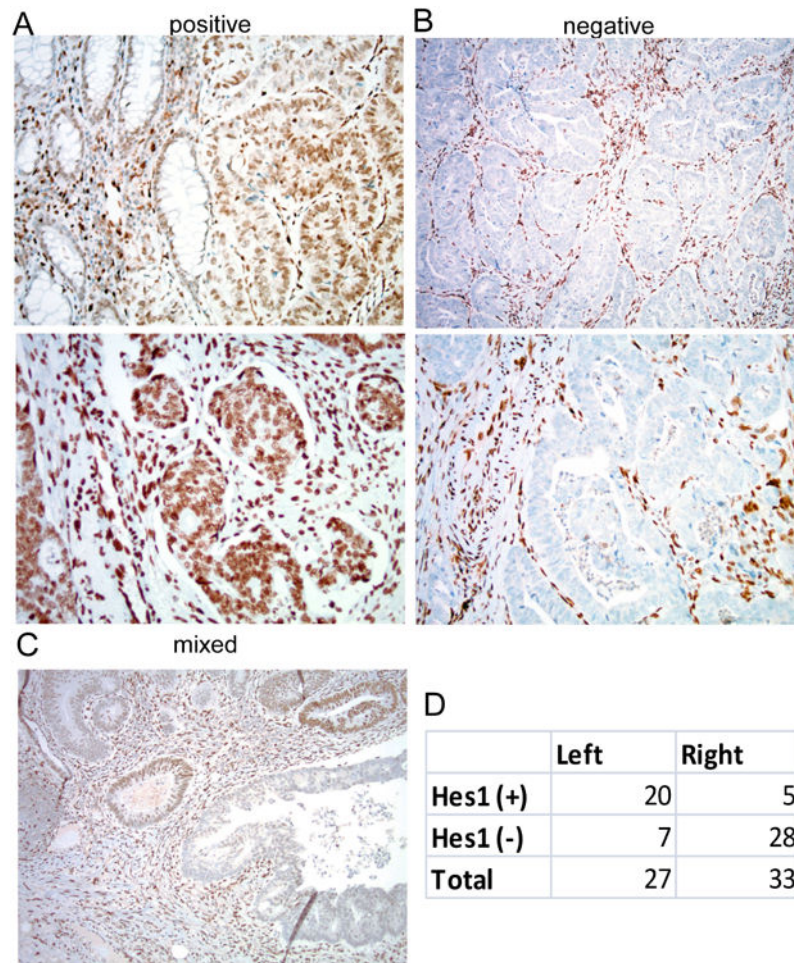


Fig 6. Loss of HES1 expression in right-sided CRC

(A-C) Representative HES1 IHC staining show 3 types of HES1 reactivity in 2 examples of positive (A) and negative nuclear reactivity (B) (top, 10 \times ; lower, 20 \times), and one mixed nuclear reactivity (C) (10 \times). (D) Summary of HES1 reactivity in 33 right- and 27 left-sided cases.

Table 1

Genotype	Diet	Donors of Bone Marrow Transplant	Antibiotics	Inflammation Score (mean)	Dysplasia Score (mean)	CAC frequency
WT	Regular*	-	-	0	0	0/5
FX ^{-/-}	On-fucose	-	-	0	0	0/16
FX ^{-/-}	Regular	-	-	14	40	14/46
FX ^{-/-}	Regular 2 months, then on fucose 30d	-	-	2	1	0/8
FX ^{-/-}	Regular	-	+	2	5	0/9
WT	Regular	WT	-	0	0	0/6
WT	Regular	FX ^{-/-}	-	1	0	0/8
FX ^{-/-}	Regular	WT	-	7	18	1/12
FX ^{-/-}	Regular	FX ^{-/-}	-	11	42	0/9***

* Regular=off-fucose diet;

*** Mice all died less than 2 months after bone marrow transfer.